307 W high-power 1018 nm monolithic tandem pump fiber source with effective thermal management

Xiaolong Chen (陈晓龙)[1], Jianhua Wang (王建华)[2], Xiang Zhao (赵 翔)[1,3], Gang Bai (柏 刚)[1,3], Weichao Gong (公维超)[1,3], Kai Liu (刘 恺)[1], Chun Zhao (赵 纯)[1], Xuan Li (李 璇)[1], Haoyang Pi (皮浩洋)[1], Jinyan Li (李进延)[4], Yifeng Yang (杨依枫)[1], Bing He (何 兵)[1,*], and Jun Zhou (周 军)[1]

[1]*Shanghai Key Laboratory of All Solid-State Laser and Applied Techniques, Research Center of Space Laser Information Technology, Shanghai Institute of Optics and Fine Mechanics, Chinese Academy of Sciences, Shanghai 201800, China*

[2]*Department of Space and Command, Academy of Equipment, Beijing 101416, China*

[3]*University of Chinese Academy of Sciences, Beijing 100049, China*

[4]*Huazhong University of Science and Technology, Wuhan 430073, China*

**Corresponding author: bryanho@siom.ac.cn*

Received February 15, 2017; accepted April 7, 2017; posted online May 5, 2017

We report a 307 W 1018 nm Yb-doped fiber laser pumped by a single 976 nm laser diode. The cavity slope efficiency is up to 75.9% and the amplified spontaneous emission is suppressed by 54 dB. The beam quality of the output laser has an M^2 factor of 1.17. Effective thermal management is considered to ensure the stable operation of our system. The power stability at the maximum output power level is measured during a period of 0.5 h and the power fluctuation is less than 0.8%. This architecture can be an effective high brightness pump source of core-pumping high-power fiber amplifiers.

OCIS codes: 140.3510, 140.3615, 140.6810, 060.2320.
doi: 10.3788/COL201715.071407.

High-power fiber lasers or amplifiers have attracted a lot of attention due to their outstanding characteristics, such as excellent beam quality, high efficiency, power scalability, and available high-power pumps[1–6]. With the development of the cladding-pumping technique, the Yb-doped fiber lasers (YDFLs) have shown 5 to 6 orders of magnitude brightness enhancement compared to that of the diode pump sources[1,7,8]. By introducing the technique of tandem pumping, YDFLs provide a new insight in available output laser power. The tandem-pumping technique refers to one or several fiber lasers pumping another one and the pump wavelength is close to the emission wavelength[9]. Compared with the cladding-pumping technique with a pump wavelength at 9xx nm, the YDFLs pumped by the tandem-pumping technique with a pump wavelength between 1000 and 1030 nm show a lower quantum defect and a reduced thermal load[10–12]. It is well known that the highest single-mode fiber (SMF) laser of 10 kW reported by IPG in 2009 was pumped by YDFLs at 1018 nm and emitted a laser at 1070 nm, and the quantum defect of less than 5% was half of that of a directly diode-pumped YDFL[13].

In recent years, a number of 1018 nm Yb-doped fiber (YDF) lasers or amplifiers have been demonstrated. Xiao *et al.*[14] reported a 77 W 1018 nm fiber laser with 15/130 μm YDF in a master oscillation power amplification (MOPA) configuration. The MOPA structure increases the complexity and instability of the whole 1018 nm tandem-pumping system. Later, they scaled the laser power to 309 and 476 W, respectively, in a fiber laser setup by using a 30 μm core diameter active fiber[15,16]. However, for the core-pumping scheme of YDFLs single-mode operation is required, and the large core diameter of 30 μm is obviously not appropriate to be applied in a core-pumping setup. For a 1018 nm SMF laser system, Ottenhues *et al.*[17] showed a 200 W output power by employing a commercially available 10/130 μm YDF. But the output power scaling needs to be further verified.

In our previous work, Li *et al.*[18] demonstrated a 7.5 W 1018 nm fiber laser. Amplified spontaneous emission (ASE) suppression was investigated, but the gain fiber had a core and cladding diameters of 20 and 400 μm which is not suitable for core-pumping applications and neither efficiency optimization nor thermal treatment were considered.

In this Letter, to present a compact high-efficiency tandem core-pumping laser source, a monolithic 1018 nm fiber laser with a total output power of 307 W is investigated. The power is much higher than the 200 W output laser power reported in Ref. [17], and the laser system is well designed to be suitable for a YDFL core-pumping setup. The gain fiber length is optimized and the slope efficiency is up to 75.9%. The ASE suppression ratio is 54 dB and no parasitic lasing is visible. The measured beam quality has an M^2 factor of 1.17. Heat dissipation of the key components is taken into account to achieve a stable laser operation. The power fluctuation is measured to be less than 0.8% of the maximum power during a measurement time of 0.5 h.

The schematic diagram of the 1018 nm fiber laser is shown in Fig. 1. The architecture consists of a single 976 nm laser diode (LD), a mode field adapter (MFA), a pair of fiber Bragg gratings (FBGs) with a reflectivity

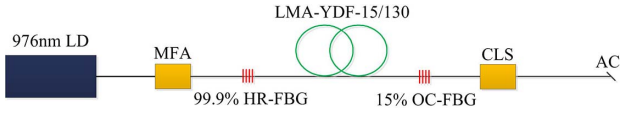

Fig. 1. Experimental setup of the 1018 nm fiber laser. LMA: large mode area.

of 99.9% (high reflectivity, HR) and 15% (output coupler, OC) at a center wavelength of 1018 nm, a length of double-clad YDF and a cladding light stripper (CLS). Thanks to the using of MFA, the pigtail fiber of 976 nm LD can be adapted to the HR FBG without using any combiners, which has been scarcely reported in other 1018 nm fiber systems. The YDF has a core/inner cladding diameter of 15/130 μm, with a cladding absorption coefficient of 11 dB/m at 976 nm. The homemade CLS is spliced at the output end of the OC FBG to filter the unabsorbed pump light from the inner cladding, and the output end of the CLS is 8° angle cleaved to suppress backward reflection. The output spectrum is measured by an optical spectrum analyzer (OSA, YOKOGAWA AQ6370) with a resolution of 20 pm.

Compared to the pump structure in Ref. [17], which consisted of a 7×1 tapered fiber bundle and five multimode pump diodes, our structure of using one pump diode connected with the HR FBG through a homemade MFA makes the system extremely compact and robust. For the MFA, the insert loss is the dominant factor to be considered. The splicing loss of multimode fibers can be predicted by the approximate formula[19]

$$\begin{cases} \Gamma_{\text{offset}} \approx 3\frac{\delta_{\text{core}}}{D_{\text{core}}} \\ \Gamma_{\text{diam}} \approx 4.5\left(1-\frac{D_{\text{core2}}}{D_{\text{core1}}}\right), \\ \Gamma_{\text{index}} \approx 1.6\left(1-\frac{\Delta_2}{\Delta_1}\right) \end{cases} \quad (1)$$

where Γ_{offset} refers to the splicing loss resulting from a lateral offset of the fibers' cores, Γ_{diam} refers to the mismatch in multimode core diameters, Γ_{index} refers to the mismatch in the fibers' cores Δ, and Δ is the relative index difference between the core and cladding. D_{core} is the core diameter, δ_{core} is the lateral offset, and the subscript 1 refers to the launching fiber and 2 refers to the receiving fiber. When the pigtail fiber of the 976 nm laser diode is spliced with the input fiber of MFA and the MFA's output fiber is spliced with the HR FBG, the fiber core is tapered from 242 to 130 μm with a <0.2 dB insert loss, which can be seen in Fig. 2.

Selecting a proper 15/130 μm YDF length considering the high cavity efficiency and effective parasitic lasing suppression, output laser spectra dependence on fiber length with consideration of ASE are theoretically simulated[20,21]. The optical spectra for active fiber lengths of 1, 1.5, and 2 m with the total output laser power of 300 W are shown in Fig. 3. It is clearly demonstrated that when the YDF length is larger than 1.5 m, strong parasitic lasing is introduced. Reducing the fiber length to 1 m, stable laser

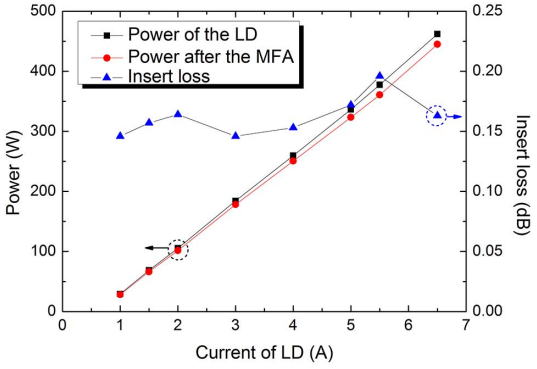

Fig. 2. (Color online) Insert loss of the MFA.

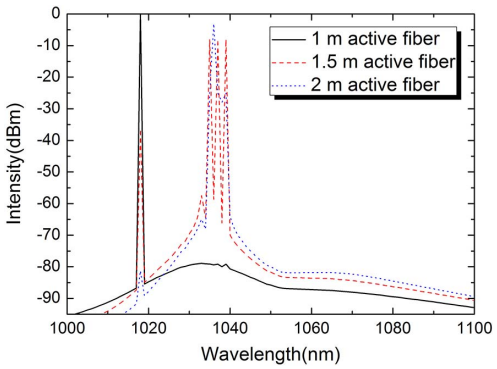

Fig. 3. (Color online) Simulated emission spectra for active fiber lengths of 1, 1.5, and 2 m.

operation at a wavelength of 1018 nm with a high ASE suppression ratio is obtained.

In order to verify the correctness of the theoretical analysis, we choose the 1.5 and 2 m YDFs to obtain the corresponding output spectra. The emission spectrum of a fiber laser with 2 m YDF is depicted in the red line of Fig. 4(a), which shows that the parasitic lasing appears obviously between 1030 and 1050 nm when the laser power is only ~30 W. However, by reducing the length of YDF to 1.5 m, the intensity of parasitic lasing is apparently weakened, even when the 1018 nm output laser reaches ~180 W, as is shown in the black line of Fig. 4(a). This phenomenon is coincident with the theoretical analysis and is because the emission cross section at 1018 nm is smaller than that at 1030 to 1080 nm while the absorption cross section at 1018 nm is larger than that at 1030 to 1080 nm. The ASE intensity at 1030 to 1080 nm is inversely proportional to the length of YDF. Since the 1.5 m YDF still cannot suppress the parasitic lasing completely, it is necessary to further decrease the length of YDF. The inserted illustration in Fig. 4(b) demonstrates the output spectrum of the 1018 nm laser with a 1.1 m YDF length. No parasitic lasing is observed and the ASE intensity is suppressed by ~54 dB, which is higher than the 50 dB suppression ratio in Ref. [17], at the maximum total output power of 307 W. The output of the 1018 nm laser power is measured as a function of the

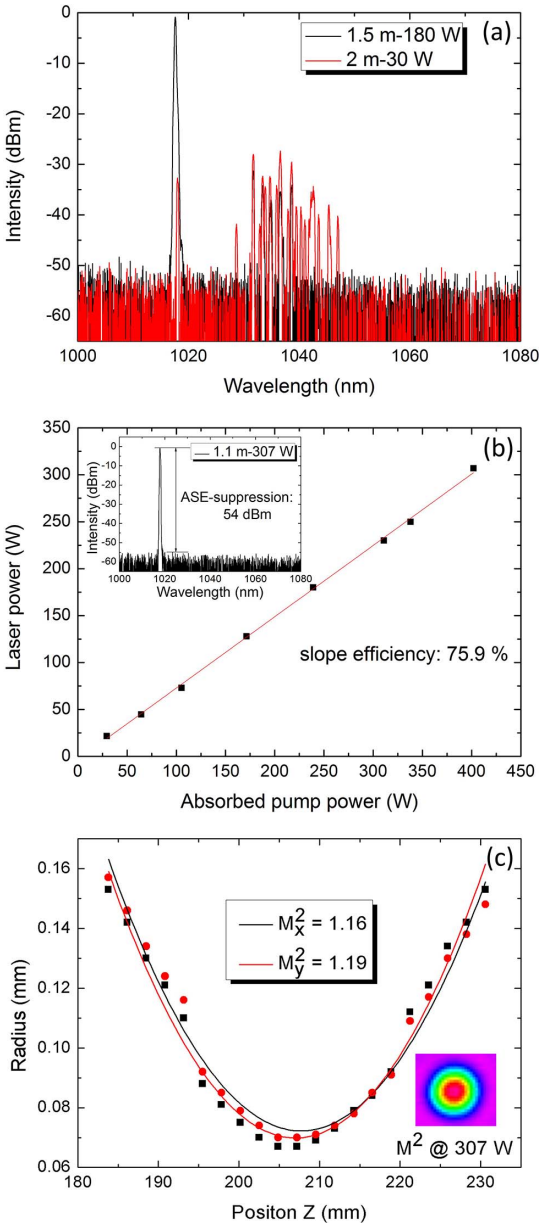

Fig. 4. (Color online) (a) Emission spectrum of 1018 nm YDF with the gain fiber lengths of 1.5 and 2 m; (b) output laser power at 1018 nm versus pump power when the gain fiber length is 1.1 m (inset is the corresponding emission spectrum); (c) beam quality evaluation.

absorbed pump power and the slope efficiency is 75.9%, higher than the 75.2% efficiency in Ref. [17], as shown in Fig. 4(b). The higher output power is limited by the available pump power. The far-field intensity distribution of the output beam is demonstrated in Fig. 4(c). The M^2 factor is directly measured by using a high-power laser quality monitor (LQM) manufactured by PRIMES. A 500 W high-power module of LQM is chosen to guarantee the 300 W-level high power test. The beam propagation direction is adjusted by a couple of reflectors with a reflectivity of >99.5% before it gets into the LQM. The M^2 factor is measured to be 1.17 and the Gaussian-like beam profile implies the suitable application for core-pumping.

It is worth noting that, in a practical application, thermal stability of key components ensures the stable operation of a-high power fiber laser. In our system, mainly heat deposition is focused on the HR FBG and the CLS. The HR FBG withstands all the input pump power. Without any specific treatment, the maximum temperature of the HR grating is up to 77.8°C as the laser power just reaches 200 W, which is shown in Fig. 5(b). In fact, low-index polymer coatings of conventional double-clad fibers are sensitive to a high thermal load and the long-term reliability may require operation below 80°C[22]. Further improving of the pump power will obviously damage the grating. A special fiber holder is designed for the HR and low reflectivity gratings, which is depicted in Fig. 5(a). The cuboid-shaped fiber holder has a thread formed groove on the surface. The width of the groove is matched with the grating's diameter of about 250 μm and the specific thread form is designed to increase the heat conducting area, which makes the heat dissipation more efficient.The grating is put in the groove and the gap is filled with thermal conductive gel. The gel has a high thermal conductivity and low optical influence. The fiber holder is cooled by a 20°C water-cooling heat sink. A carbon film with 10 μm thickness is placed between the fiber holder and the heat sink to ensure a good contact. In Fig. 5(c), we can see that by implementing the effective thermal management the maximum temperature of the HR grating is controlled to 28°C even when the 1018 nm laser power reaches 307 W.

The second component, a CLS, is needed to strip off the unabsorbed pump power in the fiber cladding. To achieve this goal, the outer cladding of the fiber is stripped over a given length, and is recoated with a material having a refractive index higher than that of the outer cladding. The

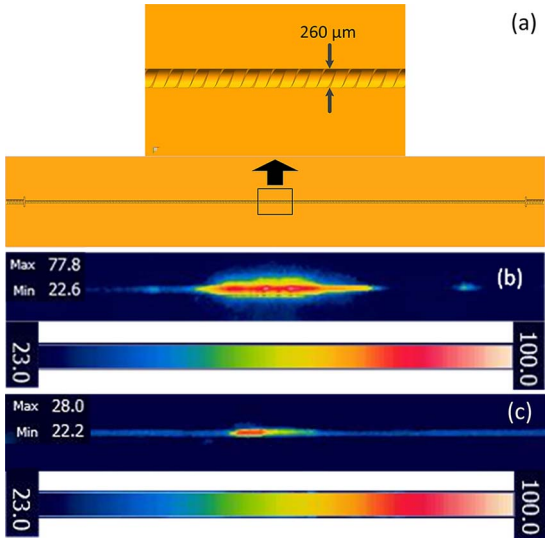

Fig. 5. Thermal management of the HR FBG. (a) Configuration of the heat sink; (b) thermal image of the HR grating with output power of 200 W and no thermal management; (c) thermal image of the HR grating with output power of 307 W and effective thermal management.

relation between attenuation and the refractive index of recoating polymers is analyzed, as is shown in Fig. 6(a). We chose three different recoating polymers along the stripper length from lower to higher indices; their refractive indices are 1.40, 1.436, and 1.54, respectively. To bring away the waste heat translated from the scattered light, a water-cooling dump is adopted in the CLS. The maximum unabsorbed pump power stripped off by the CLS is about 60 W and the highest temperature of the CLS is controlled well to 30.2°C, as is shown in Fig. 6(b).

Based on the above effective thermal control methods for FBGs and CLS, the high-efficiency hundreds-watt 1018 nm fiber laser works in a stable situation. The power stability is measured during a period of 0.5 h and the power fluctuation is less than 0.8%, as is demonstrated in Fig. 7. The surge shape fluctuation is caused by the regular change of room temperature introduced by the air conditioner.

In conclusion, a stable efficiency high-power YDFL at a wavelength of 1018 nm is reported. The compact laser system shows good robustness. A homemade YDF with a core/inner cladding diameter of 15/130 μm is employed, and the corresponding optimal gain fiber length of 1.1 m is studied theoretically and experimentally. With consideration of thermal management, the maximum output power of 307 W is obtained and the temperatures of dominant heat pots are controlled under 30.2°C. The ASE intensity is suppressed by ~54 dB and the slope efficiency is 75.9%. The power fluctuation is less than 0.8% during a period of 0.5 h. The laser system exhibits the possibility of power scaling performance and it is well designed for core-pumping applications.

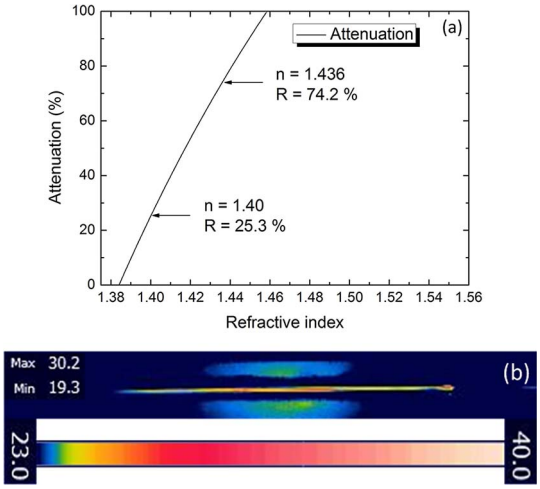

Fig. 6. Thermal management of the CLS. (a) The relation between attenuation and the refractive index of recoating polymers; (b) thermal image of the CLS with 60 W stripped off.

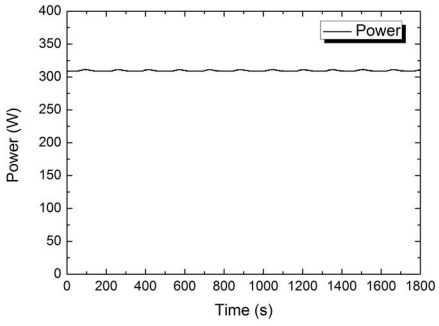

Fig. 7. Measurement of the power stability during 1800 s.

This work was supported in part by the National Key Research and Development Program of China (No. 2016YFB0402201), the National Natural Science Foundation of China (Nos. U1330134, 6130824, and 61377062), the Natural Science Foundation of Shanghai (Nos. 16ZR1440100 and 16ZR1440200), the Primary Research & Development Plan of Jiangsu (No. BE2016005-4), and the Key Project of Science and Technology of Jiangsu (No. BE2014001-2).

References

1. Y. Jeong, J. K. Sahu, D. N. Payne, and J. Nilsson, Opt. Express **12**, 6088 (2004).
2. V. Gapontsev, D. Gapontsev, N. Platonov, O. Shkurkhin, V. Fomin, A. Mashkin, M. Abramov, and S. Ferin, in *Proceedings of the Conference on Lasers and Electro-Optics Europe* (2005).
3. B. He, J. Zhou, Q. Lou, Y. Xue, Z. Li, W. Wang, J. Dong, Y. Wei, and W. Chen, Microwave Opt. Technol. Lett. **52**, 1668 (2010).
4. B. Zhao, K. Duan, W. Zhao, C. Li, and Y. Wang, Chin. Opt. Lett. **8**, 404 (2010).
5. M. Hu, Z. Quan, J. Wang, K. Liu, X. Chen, C. Zhao, Y. Qi, B. He, and J. Zhou, Chin. Opt. Lett. **14**, 031403 (2016).
6. Z. Wang, Q. Li, Z. Wang, F. Zou, Y. Bai, S. Feng, and J. Zhou, Chin. Opt. Lett. **14**, 081401 (2016).
7. Y. Jeong, A. J. Boyland, J. K. Sahu, S. Chung, J. Nilsson, and D. N. Payne, J. Opt. Soc. Korea **13**, 416 (2009).
8. J. Nilsson, in *Proceedings of the Conference on Lasers and Electro-Optics* (2010), paper CTuC1.
9. D. J. Richardson, J. Nilsson, and W. A. Clarkson, J. Opt. Soc. Am. B **27**, B63 (2010).
10. J. P. Hao, P. Yan, Q. R. Xiao, D. Li, and M. L. Gong, Chin. Phys. B **23**, 014203 (2014).
11. P. Yan, X. J. Wang, D. Li, Y. S. Huang, J. Y. Sun, Q. R. Xiao, and M. L. Gong, Opt. Lett. **42**, 1193 (2017).
12. V. Fomin, M. Abramov, A. Ferin, A. Abramov, D. Mochalov, N. Platonov, and V. Gapontsev, in *5th International Symposium on High-Power Fiber Lasers and Their Applications* (2010).
13. E. Stiles, in *5th International Workshop on Fiber Lasers* (2009).
14. H. Xiao, P. Zhou, X. L. Wang, S. F. Guo, and X. J. Xu, IEEE Photonics Technol. Lett. **24**, 1088 (2012).
15. H. Xiao, P. Zhou, X. L. Wang, X. J. Xu, and Z. J. Liu, Laser Phys. Lett. **10**, 065102 (2013).
16. X. Hu, J. Y. Leng, H. W. Zhang, L. J. Huang, J. M. Xu, and P. Zhou, Appl. Opt. **54**, 8166 (2015).
17. C. Ottenhues, T. Theeg, K. Haumann, M. Wysmolek, H. Sayinc, J. Neumann, and D. Kracht, Opt. Lett. **40**, 4851 (2015).
18. Z. Li, J. Zhou, B. He, X. Gu, Y. Wei, J. Dong, and Q. Lou, Chin. Opt. Lett. **9**, 091401 (2011).
19. A. D. Yablon, *Optical Fiber Fusion Splicing* (Springer, 2005).
20. I. Kelson and A. A. Hardy, IEEE J. Quantum Lett. **34**, 1570 (1998).
21. I. Kelson and A. A. Hardy, IEEE J. Lightwave Technol. **17**, 891 (1999).
22. M.-A. Lapointe, S. Chatigny, M. Piché, M. Cain-Skaff, and J.-N. Maran, Proc. SPIE **7195**, 719511 (2009).